

Direct Drive Permanent Magnet Synchronous Generator: Design, Modeling, and Control for Wind Energy Applications

Zina Larabi^{1,2*}, Kaci Ghedamsi³, Djamel Aouzellag³

¹ Department of Electrical Engineering, Faculty of Electrical Engineering and Computer Sciences, University of Tizi-Ouzou, P. O. B. 17 RP, 15000 Tizi-Ouzou, Algeria

² Department of Electrical Systems Engineering, Faculty of Technology, University of Boumerdes, Independence Avenue, 35000 Boumerdes, Algeria

³ Laboratoire de Maitrise des Energies Renouvelables, Faculty of Technology, University of Bejaia, Road of Targa Ouzemmour, 06000 Bejaia, Algeria

* Corresponding author, e-mail: z.larabi@univ-boumerdes.dz

Received: 09 October 2023, Accepted: 20 November 2023, Published online: 03 April 2024

Abstract

The prominent trend in wind turbine technology centers on the adoption of direct-drive permanent magnet synchronous generators (DD-PMSG), a choice driven by their capacity to deliver superior efficiency through the elimination of gearboxes. This paper presents a comprehensive exploration of the design, modeling, and control aspects of a DD-PMSG intended for harnessing wind energy conversion. Initially, the geometrical design of the generator is meticulously carried out, adhering to predefined technical specifications and constraints. Subsequently, an in-depth internal modeling, focusing on the electromagnetic behavior of the designed generator, is executed using finite element analysis (FEA) through the Ansys Maxwell RMXpert software. Finally, the external modeling and control system integration of the designed generator, connected to the grid through power electronic converters, are simulated using the Matlab/Simulink software suite. The resulting findings underscore the efficacy and viability of the proposed generator for wind turbine applications, affirming its potential to enhance wind energy conversion systems.

Keywords

design, modeling, control, wind turbine, direct drive PMSG generator

1 Introduction

In the preceding decade, the utilization of wind power within the realm of renewable energy sources has witnessed a pronounced upswing [1, 2]. In the process of converting wind energy into electrical power, two predominant categories of electrical machinery have conventionally held sway: doubly fed induction generators and synchronous generators [1]. Nevertheless, a discernible shift in practice is discernible, marked by the increasing prevalence of direct drive generators. This shift can primarily be attributed to the heightened efficiency they confer, primarily realized through the elimination of gearbox assemblies. Gearboxes have been recognized for their propensity to engender a gamut of issues, including the generation of acoustic emissions, the exigency of recurring maintenance interventions, the augmentation of energy dissipation, and a substantial contribution to system downtime rates.

The several studies presented by many authors prove that direct drive generators, especially DD-PMSG are the

best choice for wind turbines. Indeed, authors in [3] shows that the direct-drive technology offers good performance with respect to reliability, maintenance, energy extraction, and grid power quality. In [4], the authors compared five different generator systems, namely doubly-fed induction with three stages (DFIG3G) and with single-stage gearbox (DFIG1G), permanent magnet generator with single-stage gearbox (PMSG1G), direct drive generator with electrical excitation (DDSG) and direct drive permanent magnet generator (DDPMG). The authors concluded that all of the geared generators have high losses in the gearbox which reduce the energy yield, DDSG is the heaviest and most expensive alternative, and that there is important copper losses in the stator and the rotor. DDPMG does not have a gearbox and electrical excitations which reduce the losses and improve the energy yield.

The authors in [5] compared the embedded magnets with the surface mounted magnet machines. The study showed

that higher torque is achieved with surface mounted magnet machine and it needs less magnet material compared to embedded magnets. Five types of rotor structures are presented and discussed in [6] to determine the suitable rotor structure with high power for a PMSG. And it is concluded that the surface permanent magnet (SPM) structure with a magnet width/pole pitch of 90% is the most suitable rotor structure for high efficiency, low voltage, and high power output.

According to different comparisons, discussions and presentations of the direct drive generators given in the literature; our choice is focused on the design of a surface permanent magnet synchronous generator (SPMSG). It has various advantages, such as higher efficiency, larger power densities and higher reliability which reduce operation and maintenance costs.

The direct-drive generators are designed with a large diameter and small pole pitch to increase the efficiency, to reduce the active material and to keep the end winding losses small [5]. The air-gap should not exceed a few millimeters to avoid excessive magnetization requirements [5].

This paper delineates the design process of a Synchronous Permanent Magnet Synchronous Generator (SPMSG) in a structured manner, comprising three distinct sections. Firstly, we embark on an analytical design phase, entailing the meticulous calculation of the primary dimensions essential to the SPMSG. Subsequently, an internal modeling phase is executed, focusing on the intricate electromagnetic behaviors of the generator. This modeling is conducted through the utilization of Ansys Maxwell RMXpert software, facilitating a comprehensive understanding of the SPMSG's electromagnetic characteristics. Finally, the paper delves into the external modeling aspect, concentrating on the generator's performance when interfaced with the grid via a power electronic converter. This external modeling, aimed at assessing the generator's operational efficiency and behavior under practical conditions, is accomplished using Matlab/Simulink software, providing valuable insights into its grid-connected functionality.

2 Analytical design

In this section, a DD-SPMSG with 64 poles pairs, 660 kW rated power and 46.875 rpm rated mechanical speed is analytically designed. The principal dimensions of the generator are calculated using classical equations given in literature [6–13].

The geometry of the SPMSG including the parameters of the geometrical dimensions is shown in Fig. 1.

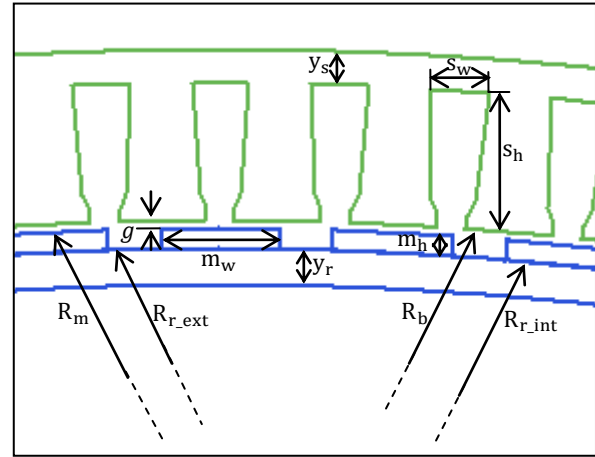


Fig. 1 Geometrical parameters of the SPMSG studied design

The bore radius (R_b) and the active length (L) of the generator are given by [6–8]:

$$R_b = \left(\frac{2r_{r1}P_n}{\pi^2 K_{w1} \hat{B}_{g1} \hat{A}_1 \Omega \cos \varphi} \right)^{1/3} \quad (1)$$

$$L = \frac{R_b}{r_{r1}} \quad (2)$$

where r_{r1} is the ratio of the radius bore to the active length (L), P_n is the rated power, K_{w1} is the stator fundamental winding factor, \hat{B}_{g1} is the fundamental air gap flux density, \hat{A}_1 is the linear current density, Ω is the rated speed and $\cos \varphi$ is the rated power factor.

The gap length (g), the stator yoke (y_s) and the rotor yoke (y_r) are expressed by [9, 10]:

$$g = 0.001 + 0.003\sqrt{R_b L} \quad (3)$$

$$y_s = y_r = \frac{\pi R_b}{2p} \frac{B_{g1}}{B_v} \alpha_m \quad (4)$$

where: p : the number of pole pairs; B_v : the flux density in the iron core; α_m : the rotor pole embrace.

The height (s_h) and the width (s_w) of the stator slot are given by [9, 11]:

$$s_h = \frac{A_1}{J_s K_r K_s} \quad (5)$$

$$s_w = \frac{\pi R_b}{Q_s} \quad (6)$$

with: J_s : the current density; K_r : the stator slot fill factor; K_s is the slot proportion; Q_s is the number of stator slots.

The height (m_h) and the width (m_w) of the permanent magnet are expressed by [7, 12, 13]:

$$m_h = K_c g \frac{\mu_r}{\frac{B_r}{\hat{B}_{g1}} - 1} \quad (7)$$

$$m_w = \frac{0.7(\pi(R_b - m_h - g))}{p} \quad (8)$$

where μ_r and B_r : the relative permeability and the residual flux density of the permanent magnet.

The imposed technical specifications and constraints which must be fulfilled by the generator are given in the Table 1, and the results calculations are summarized in the Table 2.

3 Electromagnetic analysis of the designed generator

To verify, and analyze the analytical design obtained in the Section 2, it is necessary to perform an internal modeling concerning the electromagnetic behavior of the generator. And this is done by using a finite elements method under Ansys Maxwell RMXpert software.

Table 1 Technical specifications and constraints of the SPMSG

Parameters	Symbole	Value	Unit
Rated power	P_n	660	kW
Rated speed	Ω	4.9	rad/s
Number of phases	m	3	-
Frequency	f	50	Hz
Rated power factor	$\cos \varphi$	0.95	-
Number of pole pairs	p	64	-
Linear current density	A	60e3	A/m
Surface current density	J_s	4e6	A/m ²
Winding factor	K_{w1}	0.95	-
Permanent magnet type	NdFeB	-	-
Residual flux density	B_r	1.1	T
Relative permeability	μ_r	1.05	-
Ratio of the radius bore to the active length	r_{rl}	5	-

Table 2 Design results for the SPMSG

Parameters	Symbole	Value	Unit
Bore radius	R_b	1.466	m
Active length	L	0.293	m
Stator yoke	y_s	14.4	mm
Rotor yoke	y_r	14.4	mm
Height of slot	s_h	56.7	mm
Width of slot	s_w	24	mm
Gap length	g	3	mm
Height of permanent magnet	m_h	8.7	mm
Width of permanent magnet	m_w	50	mm

3.1 Concept of the finite element method

Finite Element method (FEM) is a numerical method used in the design and analysis of all different fields in engineering (electromagnetic, mechanical, thermal...), it solves problems with complicated geometries, loading, problems with anisotropic and non linear materials and problems with time variable fields [14, 15]. The basic concept of the method (FEM) is the discretization of the model to small elements where equilibrium equations are formulated. The combination of these equations gives us the equation for the whole structure. The boundary conditions are then imposed and the equations of equilibrium are solved [16].

The magnetic field distribution in the electromagnetic systems, including electrical machine, is obtained from Maxwell's equations which described the interactions between the electric and magnetic fields [14, 15].

$$\vec{\nabla} \wedge \vec{E} = -\frac{\partial \vec{B}}{\partial t} \quad (9)$$

$$\vec{\nabla} \wedge \vec{H} = \vec{J} + \frac{\partial \vec{D}}{\partial t} \quad (10)$$

$$\vec{\nabla} \cdot \vec{D} = \rho_v \quad (11)$$

$$\vec{\nabla} \cdot \vec{B} = 0 \quad (12)$$

Adding the constitutive relationships given by [15]:

$$\vec{D} = \epsilon \vec{E} = \epsilon_0 \epsilon_r \vec{H} \quad (13)$$

$$\vec{B} = \mu \vec{H} = \mu_0 \mu_r \vec{H} \quad (14)$$

$$\vec{J} = \sigma \vec{E} \cdot \quad (15)$$

The relation Eq. (14) in a permanent magnet is given by:

$$\vec{B} = \mu_0 (\vec{H} + \vec{M}) \cdot \quad (16)$$

From Eq. (12), it implies the existence of a magnetic vector potential \vec{A} which is related to the magnetic flux density \vec{B} by:

$$\vec{B} = \vec{\nabla} \wedge \vec{A} \cdot \quad (17)$$

After calculation, the obtained magnetodynamic equation is given by:

$$\vec{\nabla} \wedge \left(\frac{1}{\mu} \vec{\nabla} \wedge \vec{A} \right) + \sigma \frac{\partial \vec{A}}{\partial t} = \vec{J}_s + \vec{\nabla} \wedge \vec{M} \cdot \quad (18)$$

In two dimensional analysis, the magnetic vector potential \vec{A} and the permanent magnets magnetization \vec{M} are reduced to the z axes scalar A_z and the (x, y) axes scalars M_x, M_y , respectively. Eq. (18) becomes:

$$\frac{\partial}{\partial x} \left(\frac{1}{\mu} \frac{\partial A_z}{\partial x} \right) + \frac{\partial}{\partial y} \left(\frac{1}{\mu} \frac{\partial A_z}{\partial y} \right) - \sigma \frac{\partial A_z}{\partial t} = -J_{sz} + \left(\frac{\partial M_x}{\partial y} - \frac{\partial M_y}{\partial x} \right) \tag{19}$$

where: μ : the magnetic permeability; ε : the electric permittivity; \vec{J}_s : the stator winding current density; σ : the electric conductivity; \vec{D} : the electric flux density; \vec{E} : the electrical field intensity; \vec{H} : the magnetic field intensity.

3.2 Maxwell 2D RMXpert model method

Firstly, the analytical design is imported to the RMXpert environment to verify it and then, to the Ansoft Maxwell 2D software to perform the magnetodynamic analysis. The geometric model of the generator under RMXpert environment is represented in Fig. 2.

The different materials selected in the RMXpert material library are: NdFe35 for the permanent magnets, Steel_1010 for the stator and the rotor core, and Copper for the stator winding. The B-H curve of the Steel_1010 is shown by Fig. 3.

A fractional double layer winding used is represented by Fig. 4. This type of winding leads to easier manufacture and lower cost of coils and the short pitching can be used to reduce cogging and certain harmonics [17].

Because of the big size of SPMSG obtained, and to minimize the simulation time, two poles of the model simulation are considered. The finite elements discretization realized in Ansoft Maxwell software is shown by Fig. 5.

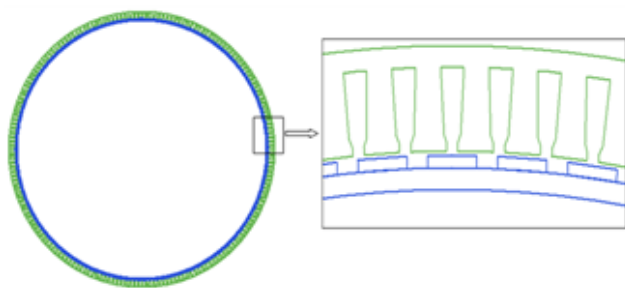


Fig. 2 SPMSG design

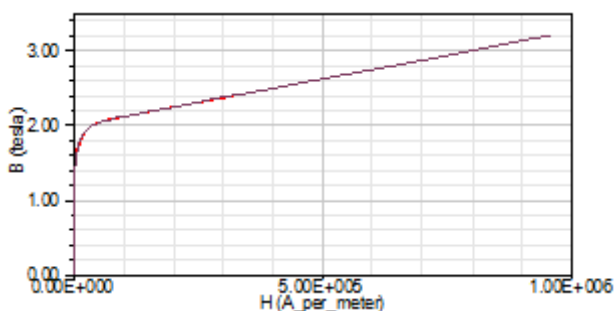


Fig. 3 B-H curve of steel_1010

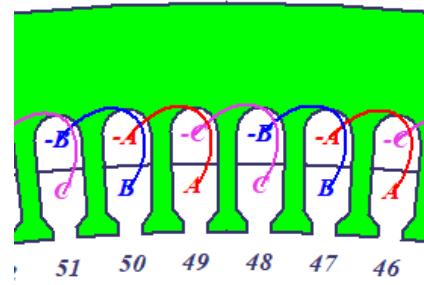


Fig. 4 Double layer fractional winding distribution

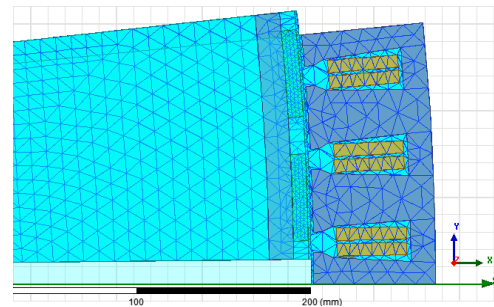


Fig. 5 Mesh analysis of the designed SPMSG

The results of the analysis of the flux lines path and the flux density distribution are shown by Figs. 6 and 7 respectively. These results are obtained at 0.4 s which correspond to the position of the rotor 113.054 degrees, and at the rated speed 46.875 rpm.

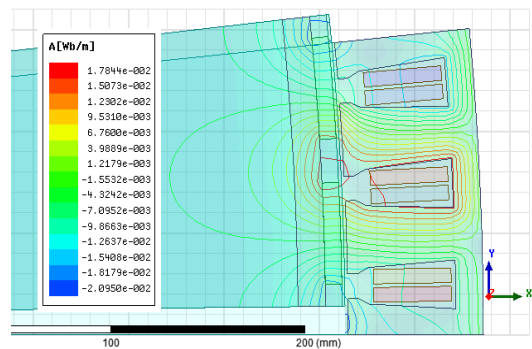


Fig. 6 Flux lines path of the designed SPMSG

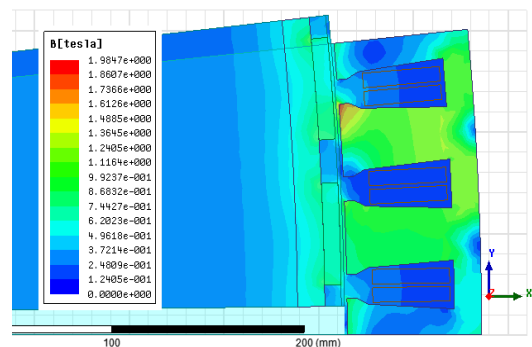


Fig. 7 Flux density distribution of the designed SPMSG

4 Modeling of the designed generator connected to the grid

The SPMSG is directly driven by the wind turbine torque (mechanical input energy) which is converted into electrical output energy [18, 19], and then injected to the grid through converter system as represented by Fig. 8.

The angular rotor speed of SPMSG is controlled via the machine side converter (MSC) to obtain the maximum wind energy [20, 21]. However, the grid side converter (GSC) is responsible for feeding of generated energy to the AC grid [20].

In this section, the modeling of the wind turbine, SPMSG and converters is carried out.

4.1 Wind turbine modeling

The extracted mechanical power from the wind (P_m) and the available turbine mechanical torque (T_m) are given by [20, 22]:

$$P_m = \frac{1}{2} \cdot \rho \cdot \pi \cdot R_T^2 \cdot C_p(\beta, \lambda) \cdot v^3 \quad (20)$$

$$T_m = \frac{P_m}{\Omega_m} \quad (21)$$

where: Ω_m : the turbine angular speed; ρ : the air density; R_T : the turbine radius; v : the wind speed; β : is the blade pitch angle; λ : is the tip speed ratio (TSR), it is given by Eq. (22):

$$\lambda = \frac{\Omega_m R_T}{V} \quad (22)$$

Concerning the power coefficient C_p , a various model are given in the literature, but in this paper a developed model given by [23] is considered. It is described by:

$$C_p = \begin{cases} C_{p_{\max}} \cdot f_{01} \cdot f_{11}; & 0 < \lambda \leq \frac{X_0}{2} \\ C_{p_{\max}} \cdot f_{02} \cdot f_{12}; & \frac{X_0}{2} < \lambda \leq X_1 \end{cases} \quad (23)$$

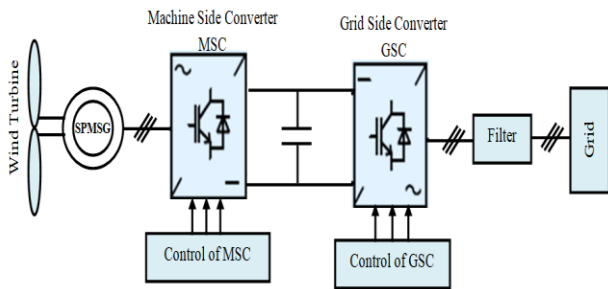


Fig. 8 SPMSG connected to the grid

with:

$$f_{01} = -\frac{4}{X_0^2} \cdot \lambda \cdot (\lambda - X_0) \quad (24)$$

$$f_{11} = e^{-\left(\frac{\lambda - \frac{X_0}{2}}{a_0}\right)^2} \quad (25)$$

$$f_{02} = -\frac{4}{(2 \cdot X_1 - X_0)^2} \cdot (\lambda - X_1) \cdot (\lambda - (X_0 - X_1)) \quad (26)$$

$$f_{12} = -\frac{2}{2 \cdot X_1 - X_0} \cdot (\lambda - X_1) \quad (27)$$

The different coefficients $C_{p_{\max}}$, X_0 , X_1 , are constant for the blad pitch angle $\beta = 0$ and they are variables for $\beta \neq 0$:

- if $\beta = 0$:

$$\begin{cases} C_{p_{\max}} = C_{p_{\max 0}} \\ X_0 = X_{00} \\ X_1 = X_{10} \end{cases} \quad (28)$$

- if $\beta \neq 0$:

$$\begin{cases} C_{p_{\max}} = C_{p_{\max 0}} - \Delta C \cdot (\beta + b \cdot \beta^\alpha) \\ X_0 = 2 \cdot \lambda_0 + \frac{8}{\beta_m^2} (\lambda_m - \lambda_0) \cdot \beta (\beta_m - \beta) \\ X_1 = \frac{X_{10}}{2 \cdot X_{00}} \cdot X_0 \end{cases} \quad (29)$$

The Table 3 [23] gives the constant parameters used for a 660 kW wind turbine [24].

The power coefficient versus lambda for different values of the pitch angle is shown in Fig. 9.

Table 3 Power coefficient parameters of a 660 kW wind turbine [23]

Parameters	Value
$C_{p_{\max 0}}$	0.49
X_{00}	15.3
X_{10}	19
a_0	11
b	0
ΔC	0.02
α	1.5
β_m	20°
λ_m	8.5
λ_0	7.65

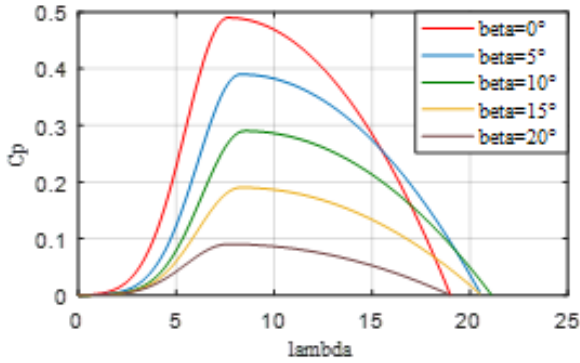


Fig. 9 Power coefficient for different values of β

4.2 Surface permanent magnet synchronous generator modeling

The mathematical modeling of the PMSG is given in the dq-axes reference frame. The stator voltage (v_d and v_q) equations are given by [24–26]:

$$\begin{cases} v_d = R_s i_d + L_d \frac{di_d}{dt} - \omega_e L_q i_q \\ v_q = R_s i_q + L_q \frac{di_q}{dt} + \omega_e (L_d i_d + \varphi_f) \end{cases} \quad (30)$$

where: R_s : the stator resistance; L_d and L_q : the d - q axis inductances; i_d and i_q : the stator currents in the d - q axis and ω_e : the electrical speed of the generator, it is related to the mechanical speed Ω_m by [24–26]:

$$\Omega_m = \frac{\omega_e}{p}. \quad (31)$$

Elsewhere, the electromagnetic torque and the mechanical equations are expressed by [24–26]:

$$T_e = \frac{3}{2} p [(L_d - L_q) i_d i_q + \varphi_f i_q] \quad (32)$$

$$T_m - T_e - f_v \Omega_m = J_{tot} \frac{d\Omega_m}{dt}. \quad (33)$$

As shown in Fig. 1, SPMSG is with smooth poles which mean that the d - q axis inductances are equal ($L_d = L_q$), the electromagnetic torque given by the Eq. (32) can be then expressed by [25]:

$$T_e = \frac{3}{2} p \varphi_f i_q \quad (34)$$

where: φ_f : the permanent magnetic flux; f_v : the friction coefficient; J_{tot} : the total mechanical inertia.

4.3 Converters modeling

As shown in Fig. 8, the generator is connected to the grid through two converters, the first one is in the machine side (rectifier) and the second one is in the grid side (inverter). The rectifier model and the inverter model are given by [27]:

$$C \frac{dV_{dc}}{dt} = (S_a i_a + S_b i_b + S_c i_c) - I_{inv} \quad (35)$$

$$\begin{cases} v_a = \frac{2S_a - S_b - S_c}{3} V_{dc} \\ v_b = \frac{2S_b - S_a - S_c}{3} V_{dc} \\ v_c = \frac{2S_c - S_a - S_b}{3} V_{dc} \end{cases} \quad (36)$$

with: C : the DC bus capacity; V_{dc} : the DC bus voltage; S_a , S_b and S_c are the control signals modulation; i_a , i_b and i_c : the phase currents of the generator, I_{inv} is the current of the inverter, v_a , v_b and v_c are the output voltage of the inverter.

5 Control of the designed generator connected to the grid

The control of the SPMSG wind turbine is briefly described in this section; it is realized by a coordinated control of the converter control and the wind turbine control.

5.1 Control of the generator side converter

From Eq. (32), it can be remarked that, the electromagnetic torque can be regulated to its reference value (T_{eref}) by acting on the q -axis current when the d -axis current is regulated to zero.

$$i_{qref} = \frac{2}{3p\varphi_f} T_{eref} \quad (37)$$

Moreover, to ensure the maximum power point tracking (MPPT) strategy, the reference generator speed (Ω_{mref}) is estimated by the optimum tip speed ratio (λ_{opt}) as follows:

$$\Omega_{mref} = \frac{\lambda_{opt}}{R} v. \quad (38)$$

As Fig. 10 shows, both d - q reference currents were transformed to their natural abc components and used for implementing the hysteresis modulation.

5.2 Control of the grid side converter

The duty of the grid side converter (GSC) is to ensure the feeding of the grid with the generated energy.

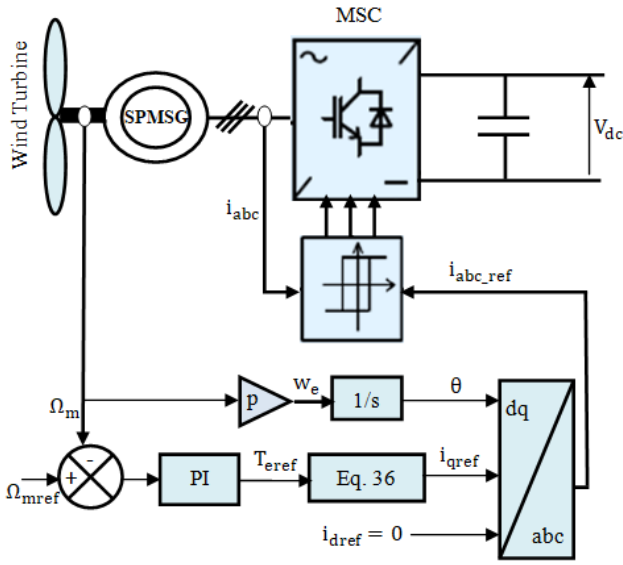


Fig. 10 Machine side converter control

The control strategy of GSC is shown in Fig. 11, where P_{gref} and Q_{gref} are the grid active power reference and the grid reactive power reference, respectively. i_{grid} is the currents grid, i_{gq_ref} and i_{gd_ref} are the d - q reference currents grid and they are calculated by [23]:

$$i_{gd_ref} = \frac{1}{v_{gq}^2 + v_{gd}^2} (P_{gref} v_{gd} + Q_{gref} v_{gq}) \quad (39)$$

$$i_{gq_ref} = \frac{1}{v_{gq}^2 + v_{gd}^2} (P_{gref} v_{gq} - Q_{gref} v_{gd}) \quad (40)$$

Both d - q grid reference currents were transformed to their natural abc components and used for implementing the hysteresis modulation.

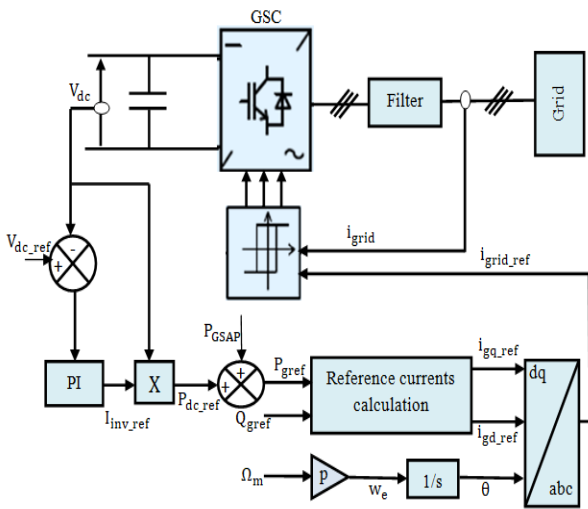


Fig. 11 Grid side converter control

6 Results and discussion

The simulation of the system described in Fig. 8 is performed with Matlab/Simulink software. The simulation parameters of the designed generator (SPMSG) and the wind turbine are given in Table 4 and Table 5 [23] respectively.

The electrical parameters of the SPMSG are calculated numerically using Ansys Maxwell RMXpert software.

The wind profile used in this study is given by Fig. 12, where the minimum value is 8 m/s and the nominal value is 12.4 m/s.

As shown in Fig. 13, the generator's mechanical speed follows the wind speed profile, reaching its rated value at the wind's nominal speed. Fig. 14 illustrates the waveform profiles of the phase current and voltage generated by the designed SPMSG. In addition, Fig. 15 shows that the active power of the generator and the grid have the same profile and variation; both have reached the optimum value (660 kW) at nominal mechanical speed. The variation of the generator's electromagnetic torque is also shown in

Table 4 SPMSG parameters

Parameters	Symbole	Value	Unit
Phase resistance	R_s	0.02	Ω
d-axis inductance	L_d	0.87	mH
q-axis inductance	L_q	0.87	mH
Generator inertia	J_g	1640.1	Kg m ²

Table 5 Wind turbine parameters [23]

Parameters	Symbole	Value	Unit
Turbine radius	R_T	19.26	m
Turbine inertia	J_T	222963	Kg m ²
Nominal mechanical speed	Ω_m	46.87	rpm
Optimum tip speed ratio	λ_{opt}	7.95	-
Maximum power coefficient	C_{pmax}	0.49	-

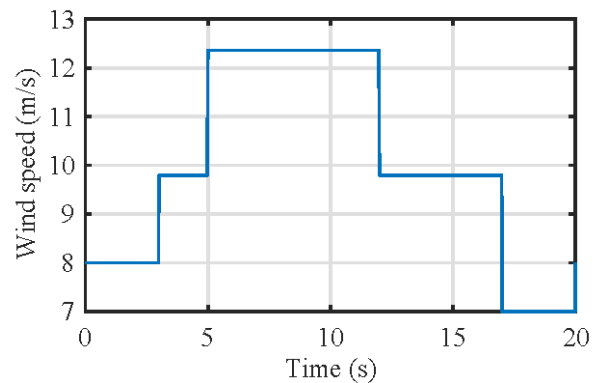


Fig. 12 Wind speed profile

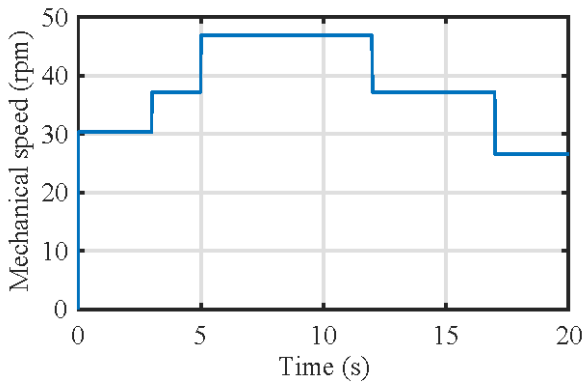


Fig. 13 Mechanical speed of the SPMSG

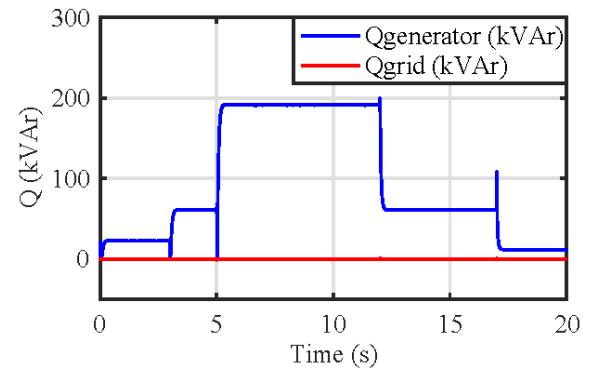


Fig. 16 Reactive power

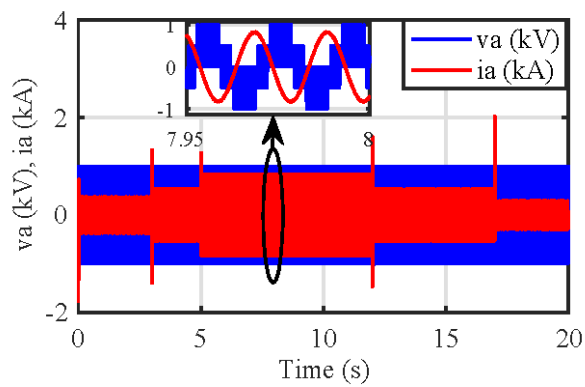


Fig. 14 Current and voltage phase of the SPMSG

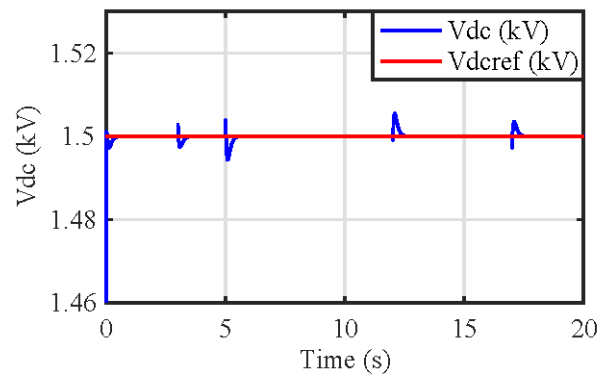


Fig. 17 DC bus voltage

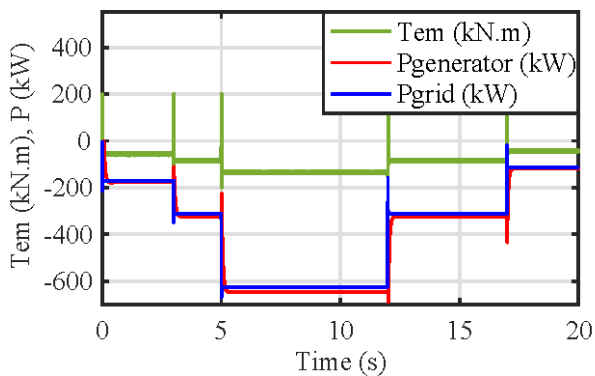


Fig. 15 Active power and electromagnetic torque

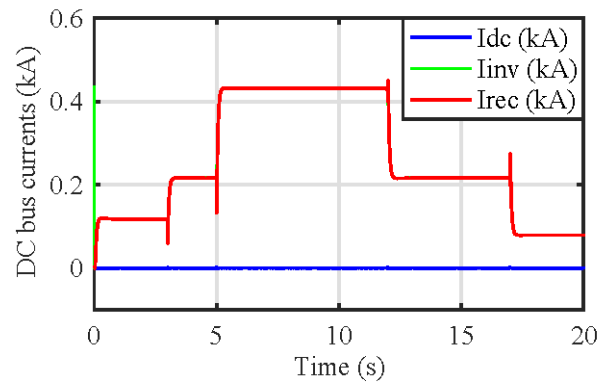


Fig. 18 DC bus currents

Fig. 15. Regarding the reactive power, it can be seen in Fig. 16 that its value is zero on the grid side, demonstrating the maintenance of the unit power factor.

Figs. 17 and 18 illustrate that the DC bus voltage is maintained at its reference and that the rectified current is identical to the current injected into the inverter. Finally, the waveform of the current and the voltage phases of the grid are shown in Fig. 19.

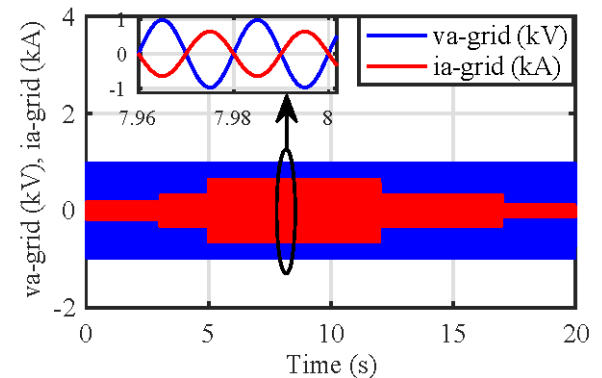


Fig. 19 Current and voltage of the grid

7 Conclusion

A Direct Drive Permanent Magnet Synchronous Generator (DD-PMSG) has been meticulously designed, thoroughly modeled, and effectively controlled for the purpose of wind energy conversion. The design phase primarily involves analytical calculations to determine the generator's key geometric parameters. Subsequently, the generator's electromagnetic behavior is rigorously verified using finite element analysis (FEA) within the Ansys Maxwell RMXpert software environment.

The integration of the designed DD-PMSG with the grid is achieved through the utilization of power electronic converters, while a precise control strategy is implemented to ensure the quality of the generated power injected into the

grid. These intricate interactions are simulated comprehensively using the Matlab/Simulink software platform.

The results obtained from these simulations exhibit a high degree of satisfaction, firmly adhering to the pre-defined technical specifications and constraints. These findings not only demonstrate the effectiveness of the designed generator for wind turbine applications but also establish its feasibility in practical scenarios.

As part of future work, a paramount objective is to bolster the credibility of the outcomes presented in this paper through experimental validation. This will involve the construction and testing of a prototype embodying the designed Synchronous Permanent Magnet Synchronous Generator (SPMSG).

References

- [1] Mohammed, Z., Muthana, A., Mohammed, R. "Sliding Mode Control of a Variable Speed Wind Energy Conversion System Using a Squirrel Cage Induction Generator", *Energies*, 10(5), 604, 2017. <https://doi.org/10.3390/en10050604>
- [2] Jean-Sola, P., McDonald, A. S., Oterkus, E. "Dynamic structural design of offshore direct-drive wind turbine electrical generators", *Ocean Engineering*, 161, pp. 1–19, 2018. <https://doi.org/10.1016/j.oceaneng.2018.04.074>
- [3] Semken, R. S., Polikarpova, M., Røyttä, P., Alexandrova, J., Pyrhönen, J., Nerg, J., Mikkola, A., Backman, J. "Direct-drive permanent magnet generators for high-power wind turbines: benefits and limiting factors", *IET Renewable Power Generation*, 6(1), pp. 1–8, 2012. <https://doi.org/10.1049/iet-rpg.2010.0191>
- [4] Polinder, H., Van der Pijl, F. F. A., De Vilder, G., Tavner, P. J. "Comparison of direct-drive and geared generator concepts for wind turbines", *IEEE Transactions on Energy Conversion*, 21(3), pp. 725–733, 2006. <https://doi.org/10.1109/TEC.2006.875476>
- [5] Salminen, P., Pyrhönen, J., Niemelä, M. "A Comparison Between Surface Magnets and Embedded Magnets in Fractional Slot Wound PM Motors", In: Wiak, S., Krawczyk, A., Trlep, M. (eds.) *Computer Engineering in Applied Electromagnetism*, Springer Dordrecht, 2005, pp. 209–214. ISBN 978-1-4020-3168-7 https://doi.org/10.1007/1-4020-3169-6_36
- [6] Haraguchi, H., Morimoto, S., Sanada M. "Suitable design of a PMSG for a small-scale wind power generator", In: *International Conference on Electrical Machines and Systems (ICEMS)*, Tokyo, Japan, 2009, pp. 1–6. ISBN 978-1-4244-5177-7 <https://doi.org/10.1109/ICEMS.2009.5382892>
- [7] Zhao, Y., Mo, C., Zhu, W., Chen, J., Wu, B., Zhang, X., Zhang, X., Chen L. "Design and Test for a New Type of Permanent Magnet Synchronous Generator Applied in Tidal Current Energy System", *Sustainability*, 15(9), 7378, 2023. <https://doi.org/10.3390/su15097378>
- [8] Ion C.P., Calin M. D., Peter I. "Design of a 3 kW PMSM with Super Premium Efficiency", *Energies*, 16(1), 498, 2023. <https://doi.org/10.3390/en16010498>
- [9] Abdeljalil, D., Chaieb, M., Benhadj, N., Krichen, M., Neji, R. "Design and optimization of permanent magnet synchronous generator dedicated to direct-drive, high power wind turbine", *Wind Engineering*, 46(3), pp. 737–758, 2022. <https://doi.org/10.1177/0309524X211046379>
- [10] Paul, S., Chang, J. "Model-based design of variable speed non-salient pole permanent magnet synchronous generator for urban water pipeline energy harvester", *International Journal of Electrical Power & Energy Systems*, 125, 106402. 2021. <https://doi.org/10.1016/j.ijepes.2020.106402>
- [11] Akyün, Y., Nory, H., Talas, M., Kürüm, H. "Design Analysis and Verification of PMSM Motor For Dishwasher Machine", In: *International Conference on Power Electronics and their Applications (ICPEA)*, Elazig, Turkey, 2019, pp. 1–7. ISBN 978-1-7281-2726-2 <https://doi.org/10.1109/ICPEA1.2019.8911146>
- [12] Nicorici, A. M., Szabo, L., Martis, C. "Design and Analysis of a Permanent Magnet Synchronous Machine used in Automotive Applications", In: *2019 IEEE International Conference on Environment and Electrical Engineering and 2019 IEEE Industrial and Commercial Power Systems Europe*, Genova, Italy, 2019, pp. 1–6. ISBN 978-1-7281-0653-3 <https://doi.org/10.1109/EEEIC.2019.8783826>
- [13] Arslan, S., Kurt, E., Akizu, O., Lopez-Guede, J. M. "Design optimization study of a torus type axial flux machine", *Journal of Energy Systems*, 2(2), pp. 43–56, 2018. <https://doi.org/10.30521/jes.408179>
- [14] Stoev, B., Todorov, G., Rizov, P., Pagiatakis, G., Dritsas, L. "Finite Element Analysis of Rotating Electrical Machines—An Educational Approach", In: *2017 IEEE Global Engineering Education Conference (EDUCON)*, Athens, Greece, 2017, pp. 262–269. ISBN 978-1-5090-5467-1 <https://doi.org/10.1109/EDUCON.2017.7942857>

- [15] Bianchi, N. "Electrical Machine Analysis Using Finite Elements", CRC Press, 2005. ISBN 9781315219295
<https://doi.org/10.1201/9781315219295>
- [16] Khoshkar, H. F., Doroudi, A., Mohebbi, M. "Finite Element Analysis of Permanent Magnet Synchronous Motors Subjected to Symmetrical Voltage Sags", Iranian Journal of Electrical and Electronic Engineering, 10(4), pp. 333–340, 2014. [online] Available at: <https://ijeee.iust.ac.ir/article-1-637-en.html> [Accessed: 09 September 2023]
- [17] Kundrotas, B., Petrovas, A., Rinkeviciene, R., Smilgevicius, A. "Research of Six-Phase Induction Motor Windings", Elektronika ir Elektrotechnika, 20(1), pp. 15–18, 2014.
<https://doi.org/10.5755/j01.eee.20.1.2237>
- [18] Htet, T. Z., Zhao, Z., Gu Q., Li, J. "Modelling and Analysis of Radial Flux Surface Mounted Direct-Driven PMSG in Small Scale Wind Turbine", Advances in Science, Technology and Engineering Systems Journal., 2(6), pp. 94–99, 2017.
<https://doi.org/10.25046/aj020612>
- [19] Fazli, N., Siahbalaee, J. "Direct Torque Control of a Wind Energy Conversion System with Permanent Magnet Synchronous Generator and Matrix Converter", In: 2017 8th Power Electronics, Drive Systems & Technologies Conference (PEDSTC), Mashhad, Iran, 2017, pp. 166–171. ISBN 978-1-5090-5766-5
<https://doi.org/10.1109/PEDSTC.2017.7910315>
- [20] Gajewski, P., Pieńkowski, K. "Analysis of Sliding Mode Control of Variable Speed Wind Turbine System With PMSG", In: 2017 International Symposium on Electrical Machines (SME), Naleczow, Poland, pp. 1–6. ISBN 978-1-5386-0359-8
<https://doi.org/10.1109/ISEM.2017.7993554>
- [21] Thongam, J. S., Tarbouchi, M., Beguenane, R., Okou, A. F., Merabet, A., Bouchard, P. "A Power Maximization Controller for PMSG Wind Energy Conversion Systems", Journal of Electrical and Control Engineering, 3(6), pp. 1–8, 2013.
- [22] Hallouz, M., Kabeche, N., Moulahoum, S., Kechidi, Z. "Experimental Investigation of DFIG-based Wind Energy Conversion System Using Fuzzy Logic Control", Periodica Polytechnica Electrical Engineering and Computer Science, 67(3), pp. 260–267, 2023.
<https://doi.org/10.3311/PPee.21233>
- [23] Laverdure, N. "Sur l'Intégration des Générateurs Eoliens dans les Réseaux Faibles ou Insulaires" (On the Integration of Wind Turbine Generators into Weak or Insular Grids), Phd Thesis, Polytecnic National Institute of Grenoble, France, 2005. [online] Available at: <https://theses.hal.science/tel-00170128> [Accessed: 02 September 2023] (in French)
- [24] Belaid, S., Rekioua, D., Oubelaid, A., Ziane, D., Rekioua, T. "Proposed Hybrid Power Optimization for Wind Turbine/Battery System", Periodica Polytechnica Electrical Engineering and Computer Science, 66(1), pp. 60–71, 2022.
<https://doi.org/10.3311/PPee.18758>
- [25] Errami, Y., Obbadi, A., Sahnoun, S., Oussaid, M., Maaroufi, M. "Power Extraction Control of Variable Speed Wind Turbine Systems Based on Direct Drive Synchronous Generator in all Operating Regimes", Journal of Electrical and Computer Engineering, 2018(3), pp. 1–17, 2018.
<https://doi.org/10.1155/2018/3837959>
- [26] Mazouz, L., Zidi, S. A., Hafafa, A., Hadjeri, S., Benaissa, T. "Optimal Regulators Conception for Wind Turbine PMSG Generator Using Hooke Jeeves Method", Periodica Polytechnica Electrical Engineering and Computer Science, 63(3), pp. 151–158, 2019.
<https://doi.org/10.3311/PPee.13548>
- [27] Camara, M. S., Camara, M. B., Dakyo, B., Gualous, H. "Modélisation et commande d'une génératrice synchrone à aimant permanent pour la production et l'injection de l'énergie offshore dans un réseau" (Modeling and control of a permanent magnet synchronous generator for offshore power generation and grid injection), In: Francophone Electrical Engineering Symposium, Cachan, France, 2014, pp. 8–10.